EXPERIMENTAL INVESTIGATION OF THE INCREMENTAL CONDUCTANCE MPPT ALGORITHM AT HIGH PERTURBATION RATES

M. A. Elgendy[1], D. J. Atkinson[1] and B. Zahawi[2]

[1]School of Electrical and Electronic Engineering, Newcastle University, Newcastle upon Tyne, NE1 7RU, United Kingdom.

[2]Department of Electrical and Computer Engineering, Khalifa University, Abu Dhabi 127788, UAE

Keywords: DC-DC power conversion, Incremental Conductance algorithm, maximum power point tracking, photovoltaic power systems.

Abstract

One of the most commonly utilized maximum power point tracking (MPPT) algorithms for photovoltaic (PV) generators is the Incremental Conductance (INC) algorithm. Yet, the operating characteristics of this algorithm at high perturbation frequencies, when the system response to MPPT perturbations is never allowed to settle, have not been addressed in the literature. This paper characterizes system behaviour in this operating mode experimentally for a standalone PV system with a motor-pump load (and a resistive load). Results show that the INC algorithm operating at a high perturbation rate offers higher energy utilization efficiency and better system performance despite the resulting non-periodic waveforms of the system.

1. Introduction

A variety of MPPT algorithms with different levels of complexity, efficiency and implementation costs, have been proposed in the literature for maximizing the energy utilization efficiency of PV arrays [1, 2]. The simplest method to maintain operation at/or near the maximum power point (MPP) is to operate the PV array at a constant voltage equal to its MPP voltage provided by the manufacturer. The energy utilization efficiency can be significantly improved at little extra cost by using a hill climbing MPPT technique such as the Perturb and Observe (P&O) algorithm or the incremental conductance (INC) algorithm. The operation of the INC algorithm [3-9] is based on the fact that the power-voltage curve of a photovoltaic array has one MPP for a given cell temperature and solar irradiance level, as shown in Fig.1. At this MPP, the derivative of the power with respect to the voltage equals zero which means that the sum of the instantaneous conductance (I_{PV}/V_{PV}) and the incremental conductance (dI_{PV}/dV_{PV}) equals zero. The sum of the instantaneous conductance and the incremental conductance is positive on the left hand side (LHS) of this MPP while it is negative on the right hand side (RHS) of the MPP. The algorithm compares the incremental conductance of a PV array with its instantaneous conductance [9] and makes a decision as to increase or decrease a certain control parameter by a small amount (step size).

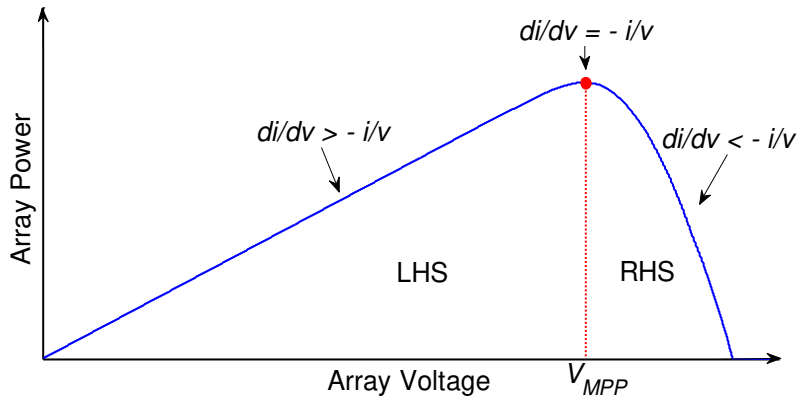

Fig. 1. Power-voltage characteristic of a PV array

Two techniques are available for implementing the INC algorithm: reference voltage control [9, 10] and direct duty ratio control [11, 12]. In reference voltage control, a PI controller is employed to vary the duty ratio of the MPPT converter using the array output voltage as a control parameter. For direct duty ratio control, the control parameter is the duty ratio of the converter. The control parameter is continually perturbed, at a chosen rate and step size, even when the array is operating under constant temperature and solar irradiance conditions. If the perturbation rate is low and the step size is high, system waveforms in the steady state fluctuate between three levels around their MPP values. The relatively high step sizes used to achieve three-level operation result in large steady-state oscillations and a decrease in the energy utilization efficiency of the system. Steady-state oscillations can be reduced by using lower step sizes. However, this slows down the starting transient of the MPPT algorithm and the response of the system to changes in weather conditions. The slow transient response can be compensated for by using an adaptive step size scheme [12-15], however, this may require higher computational complexity and/or need system dependent constants.

The slow transient response can also be addressed by using a higher perturbation frequency. If the perturbation rate is increased so that the sampling period becomes shorter than the settling time, the system will never reach a steady state. The interaction between system dynamics and the MPPT perturbations results in quasi-periodic system waveforms (i.e. with an oscillation frequency much lower than the perturbation frequency). With reference voltage perturbation, this interaction may result in PI controller instability and thus loss of MPP tracking (similar to that observed with the P&O algorithm when operated at a high perturbation frequency [16]). However, with direct duty ratio perturbation, variations in system waveforms around the MPP are always bounded and the global stability of the system is preserved.

The performance of the INC algorithms at low perturbation rates has been the subject of numerous studies in the literature. However, its performance at high perturbation rates when system response to MPPT perturbations is never allowed to settle has not been given any attention. This

omission is addressed in this paper which investigates the operating characteristics of the INC algorithm when employed with direct duty ratio perturbation at a high perturbation rate. A standalone PV systems (operating with a resistive load and with a motor-pump load) is considered in this study using a 1080-Wp site installation. PV array emulators are not suitable for evaluating MPPT algorithms in this operation mode because of the very short perturbation intervals used at high perturbation rates. The qualitative and quantitative behavior of the systems is evaluated experimentally and by numerical simulations. Comparisons are made with previously published results [8] obtained from the same test site using the INC algorithm when operated at low perturbation rates. The comparison shows that the INC algorithm offers excellent energy utilization and faster recovery of the MPP in rapidly changing irradiance conditions when operated at high perturbation rates, despite the aperiodic nature of system waveforms in this mode of operation.

2. System Description

A PV system employing switching converters for MPPT control is a highly nonlinear time-varying system. In addition to the nonlinear source (PV array characteristics) and load (pump characteristics), the system includes two other sources of nonlinearity which are the switching action of the power electronic converter and the nonlinear MPPT control of the INC algorithm. For three-level operation, the perturbation interval is very long compared to the switching cycle of the converter. In this case, it is possible to take the averages of different variables over a switching cycle and to linearize nonlinear functions about the operating point using Taylor's series expansion. The linearized averaged model can be solved analytically to predict the response of the system to a single MPPT perturbation, i.e. a small perturbation in duty ratio. The analytical model can then be used for the next perturbation after updating the initial conditions and so on. A full derivation of the analytical solution and a comprehensive stability analysis of the system have already been presented by the authors in [17].

At high perturbation rates however, the sampling interval is very short so that the switching action of the converter cannot be neglected. Similarly, the effect of the nonlinear (flowchart-based) operation of the INC algorithm cannot be neglected as the system will never have enough time to reach an equilibrium point before the next perturbation. The averaged linearized model is no longer valid and it is impossible to find a closed form analytical solution similar to that of the three-level operation mode. For this reason, system operation at high perturbation rates is characterized experimentally in this paper.

The experimental rig used in this investigation (which was also used and presented in some past investigations of the authors including [16, 17]) is comprised of a roof-installed 1080-Wp array, a step down dc–dc converter and a dc motor/pump load. Investigations were also carried out for a 40Ω resistive load fed through a 2.2mH-100μF LC low pass filter. Very similar system waveforms were obtained with the resistive load when the INC algorithm is employed at a high perturbation rate and these are not shown in this paper because of space limitations. The array consists of two parallel branches of three series connected SANYO HIP-J54BE2, 180-Wp solar modules. Meteorological parameters were measured and recorded at one second intervals using a roof-top weather station installed alongside the PV array. Hall Effect sensors were used to measure array voltage and current. A Texas Instruments TMS320F2812 digital signal processor (DSP) based eZdsp kit was used for control implementation and data acquisition purposes. A high performance DSP was employed in the test rig for experimental flexibility and ease of programming. However, a low cost microcontroller would have been more than adequate to implement the INC control algorithms under investigation. Motor armature inductance and resistance values were measured at 3.5mH and 1.25Ω, respectively. The converter PWM switching frequency was fixed at 10kHz, an appropriate choice for the IGBT switch used in the MPPT converter based on converter efficiency considerations. A commercial dc link capacitor of 470μF with the required current ripple capability was used to store the generated energy during the IGBT switch off-periods. With these parameter values, continuous current mode

operation was achieved. A simplified circuit diagram of this system with the motor-pump load is shown in Fig. 2. The same experimental site test rig was used in some past investigations of the authors including [16, 17].

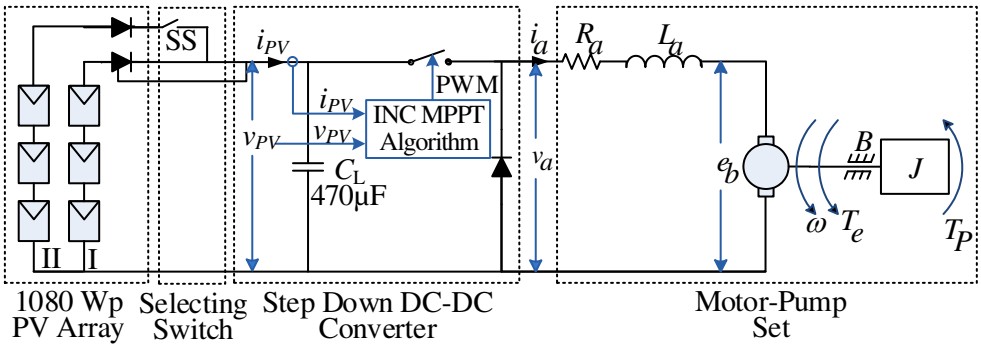

Fig. 2. Simplified circuit diagram of experimental PV pumping system

To study the starting and steady-state performance of the algorithm, the experimental system was operated at constant weather conditions for a period of 30 seconds, using a sampling rate of 2K samples/sec to measure and record the various parameters of the system. A longer test duration of 20min was used to calculate the energy utilization efficiency at different weather conditions and to examine the effects of variations in weather conditions on system behavior. A lower sampling rate of 10 Samples/sec was used in this longer duration test to limit the storage requirement and computer buffer size. A numerical simulation of the system was also developed using the measured characteristics of each individual component of the experimental system [18]. These simulations were used to identify the appropriate range of step sizes of the algorithm. Simulations were also used to study the effects of step changes in irradiance level on the behavior of the algorithm as this cannot be carried out experimentally with a site installed PV array.

3. System Waveforms

The continuous perturbations of the INC algorithm result in steady-state fluctuations in system waveforms. Fig. 3a shows the system waveforms calculated at 1000W/m^2 solar irradiance and 25˚C

cell temperature using a step size of 5% and a low perturbation rate of 1Hz. At this low perturbation rate, the sampling interval is long enough to allow the response to settle before the next perturbation and the waveforms fluctuate between three levels around their MPP values, as shown. Fig. 3b shows the waveforms of the system at the same irradiance and temperature conditions when operated with a perturbation rate of 2kHz (the same as the analogue to digital conversion (ADC) rate) and a step size of 0.05%. At such a high perturbation rate, the perturbation period is shorter than the settling time of the system. Because of this, the INC algorithm continues to decrease/increase the duty ratio beyond its optimum value. As a result, the duty ratio (and consequently the array voltage and current) oscillate around the MPP in a quasi-periodic pattern (with the oscillation frequency being much lower than the perturbation frequency), causing the array power to fall slightly below the maximum possible value. All system waveforms are always bounded by two levels and the system is globally stable.

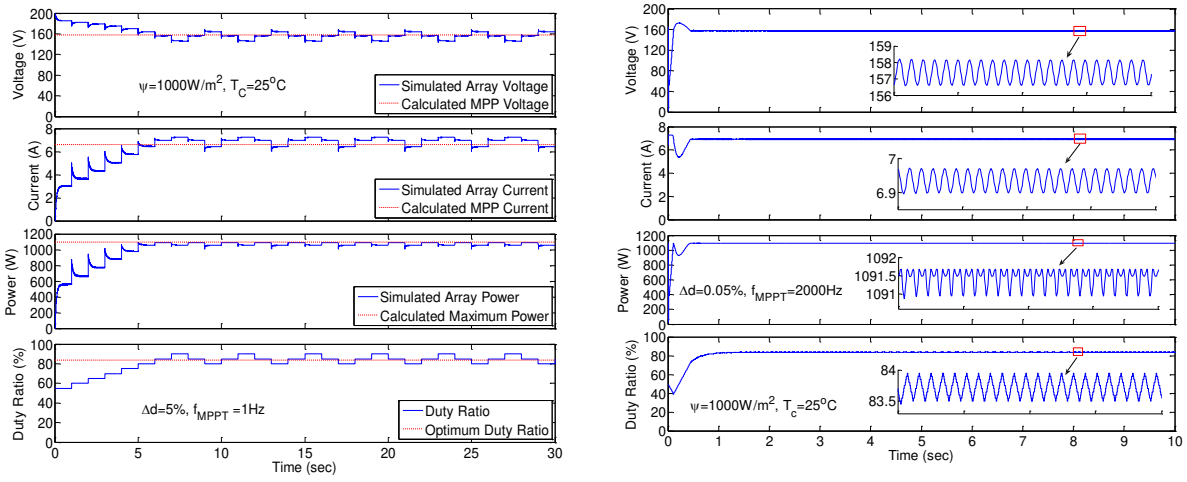

(a) (b)

Fig. 3. Simulated system response; (a) three-level operation, (b) high perturbation rate.

To demonstrate the dynamic behavior of the INC algorithm when operated in this high perturbation rate mode, a short interval of the voltage, power and duty ratio plots of Fig. 3b is magnified and shown in Fig. 4. Evert time the MPP is crossed, the sign of the differential dP_{PV}/dV_{PV}

changes and the direction of perturbation is reversed. The duty ratio decreases when the operating point is on the positive slope of the power-voltage curve (time intervals X in Fig. 4) and increases when it is on the negative slope part (time intervals Y in Fig. 4).

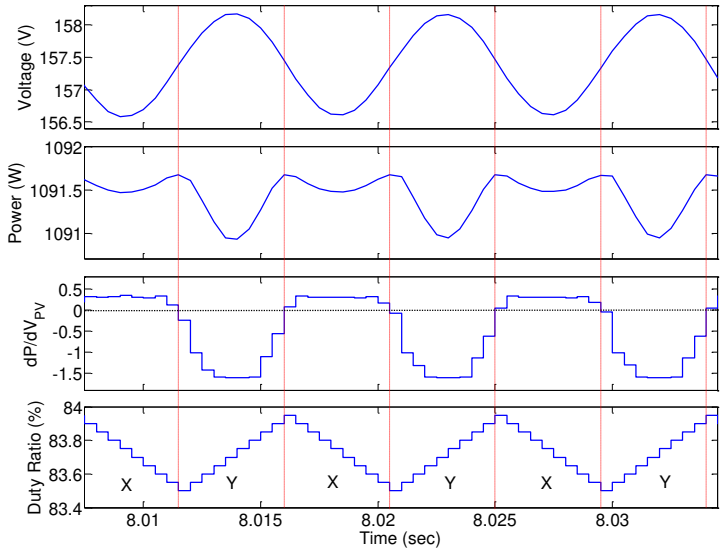

Fig. 4. Dynamic behavior of INC algorithm at a high perturbation rate

Fig. 5 shows the duty ratio–array voltage phase portrait of the system, sampled at the perturbation frequency. When the MPP is crossed at point A, a negative dP_{PV}/dV_{PV} is obtained and the algorithm increases the duty ratio accordingly. Normally, it would be expected that increasing the duty ratio would decrease the array voltage, moving the operating point back towards the MPP at point A. However, due to the difference in speed between the system response and INC algorithm perturbations, the array voltage continues rising even while increasing the duty ratio, reaching a maximum value of 158.14V at point B where it starts to respond to the duty ratio increase. The MPP is not reached at the calculated optimal duty ratio of 83.61% but at a higher duty ratio of 83.95% instead. When crossing the MPP to the LHS at point C, the algorithm reverses the duty ratio perturbation direction decreasing the duty ratio. Again, the array voltage does not respond immediately but continues reducing until a minimum value of 156.64V is reached at point D where

the system starts to respond to the decrease in duty ratio. The MPP is reached at point A again at a minimum duty ratio of 83.5%, and the sequence is repeated until the irradiance changes. Similar bounded phase portraits indicative of a globally stable quasi-periodic system [19, 20] are obtained for other combinations of system state variables.

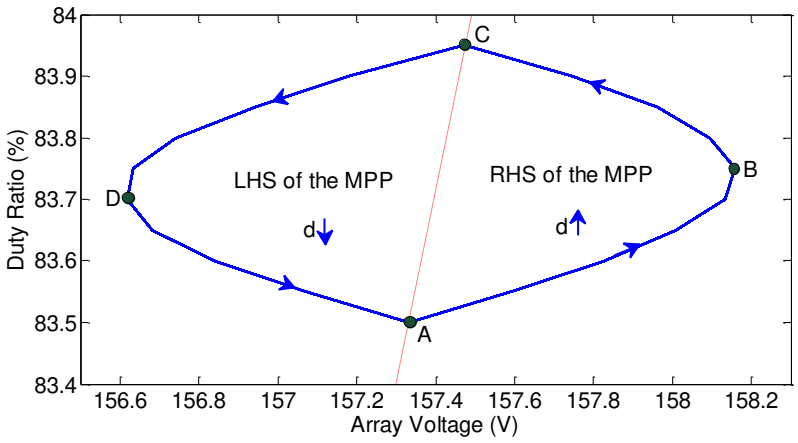

Fig. 5. Sampled duty ratio−array voltage phase portrait

4. Choice of Algorithm Parameters

When the INC algorithm is employed in its conventional three-level mode of operation, the perturbation period is chosen to be higher than the settling time of the system to a single MPPT perturbation. The step size is then chosen so that low steady-state oscillations are achieved with good transient characteristics. For operation at a high perturbation rate, the perturbation frequency can be set at its maximum possible value equal to the ADC rate of the array voltage and current. This will facilitate the implementation of the algorithm as the duty ratio can now be updated at the same rate as the measured parameters. Once the perturbation frequency has been chosen, there remains only one parameter to be selected; the step size at which the duty ratio of the MPPT converter is perturbed.

In this paper, the duty ratio/array voltage bifurcation diagram is calculated and used as a design tool for defining the appropriate step size of the INC algorithm. The term “bifurcation” represents a qualitative change in system dynamics which occurs as a system parameter is varied [19, 20]. The

bifurcation diagram gives a global view of the effect of the bifurcation parameter on system performance and can thus be used to identify the appropriate range of that particular parameter during the design stage.

Fig. 6 shows the array voltage/step size bifurcation diagram of the system at 1000W/m^2 solar irradiance and 25˚C cell temperature. This diagram is obtained by taking 300 samples of the steady-state array voltage at the perturbation rate (2kHz) for each value of the step size. The 300 samples of the array voltage at each step size value are spread around the MPP voltage (157.58V). The magnitude of the array voltage oscillation is nearly unchanged for a step size up to about 0.07%. However, the higher the step size the faster the transient response of the system and the lower the impact of noise on MPPT algorithm decisions. For these reasons, a step size between 0.04% and 0.07% (Fig. 6) would be an appropriate choice for the PV pumping system considered in this study. Above a step size of 0.07%, the magnitude of the array voltage oscillations increases with the increase in step size resulting in high magnitude quasi-periodic array voltage oscillations. This will result in higher swings in system waveforms around the MPP values and thus low tracking efficiency and undesired motor operation. Similar bifurcation diagrams were obtained for motor current and speed.

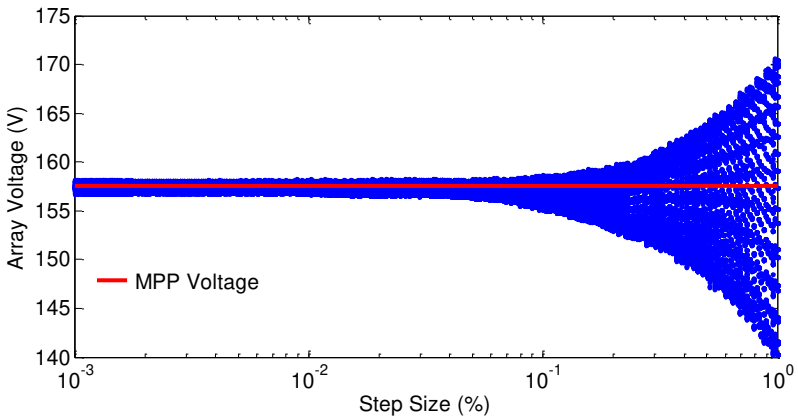

Fig. 6. Array voltage−step size bifurcation diagram

5. Effects of Noise on Algorithm Operation

For an actual site installation operating with a high perturbation rate and low step size, the INC algorithm may easily be confused due to noise. Fig. 7 shows the array voltage, current, power and the duty ratio waveforms of the experimental system operating at a high perturbation rate equal to the ADC rate (2kHz). Algorithm confusion due to noise changes the perturbation direction before the MPP is crossed producing non-periodic system waveforms (unlike the quasi-periodic waveforms obtained from the simulation which does not take noise into account). This is not a significant problem in this case however, because even if the algorithm is confused due to noise, the perturbation direction would be corrected after a very short time (due to the very short perturbation intervals). Even with presence of noise, the steady-state oscillation in system waveforms is lower than the three-level operation case. It worth mentioning that, with high perturbation rates, no low pass filters were used for the voltage and current signals. In this case, the delay of such filters is comparable to the MPPT sampling interval (perturbation interval) and thus may result in confusion to the INC algorithm. This is unlike the three-level operation case where filter delay is negligible compared to the MPPT sampling time [16]. To verify that noise is the main reason for not obtaining quasi-periodic waveforms in the experimental system, noise signals (obtained by measuring the voltage and current waveforms of the experimental system while the pump and array were disconnected) were added to the array current and voltage feedback signals in the simulation before being processed by the INC algorithm. The resulting waveforms (Fig. 7.b) are non-periodic similar to those obtained from the experimental system (Fig. 7.a) at the same weather conditions.

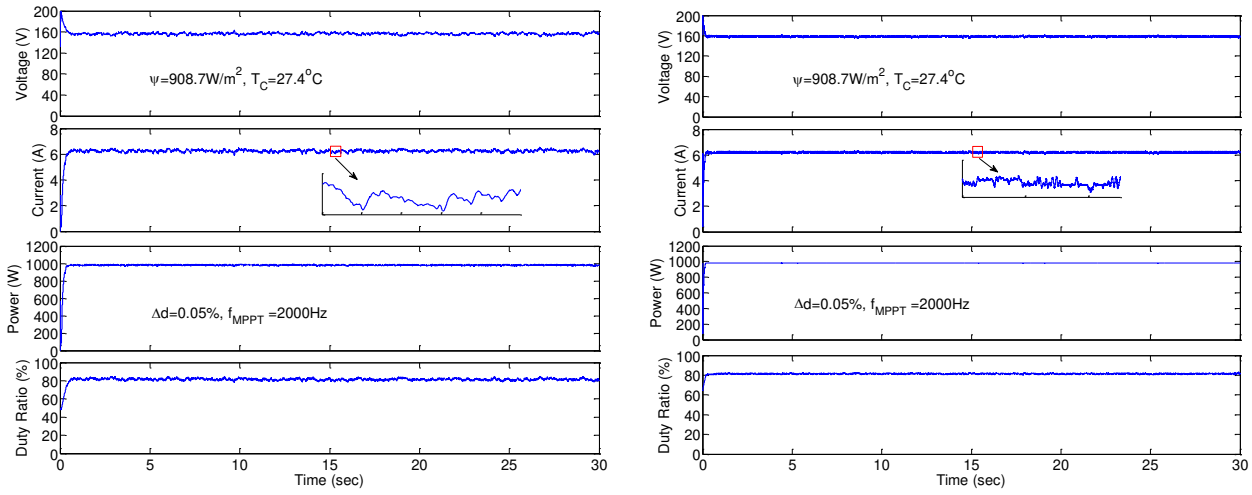

(a) (b)

Fig. 7. Effects of noise on algorithm operation at a high perturbation rate; non-periodic waveforms, (a) experimental results, (b) simulation results

6. Confusion due to Changes in Irradiance Levels

At low perturbation rates, the INC algorithm may be confused during periods of solar irradiance changes. The time required by the algorithm to move the operating point to oscillate around the new MPP depends on the step size, the perturbation frequency and the rate and magnitude of the irradiance change. When operated at a high perturbation rates, the INC algorithm is frequently confused by system dynamics, but it has a much faster transient response compared to when it's operating at lower perturbation rates. Fig. 8 shows the simulated duty ratio responses for step irradiance changes from 500W/m^2 to 1000W/m^2 and from 1000W/m^2 to 500W/m^2. The duty ratio follows its optimum value with a small delay of less than 1s due to the dc motor electrical time constant (L_a/R_a) and algorithm confusion by system dynamics. With three-level operation, the duty ratio is updated at a much slower rate due to the large sampling interval. In this case, the response of the INC algorithm to the same step irradiance change is much slower, as reported in [8].

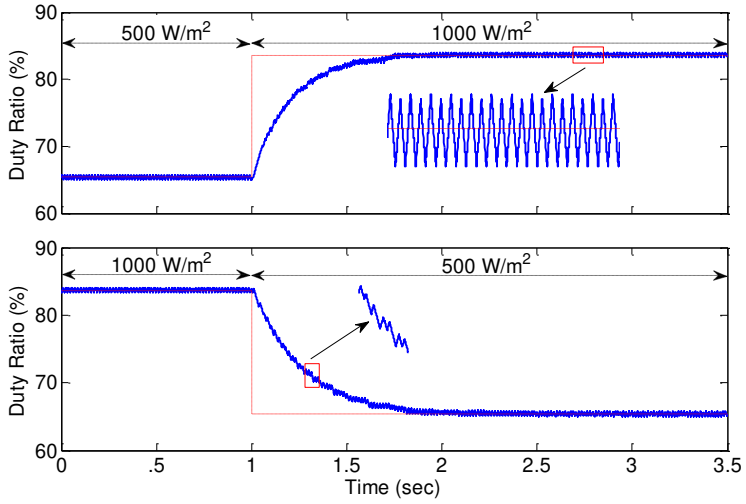

Fig. 8. Simulated response of the INC algorithm to a step change in solar irradiance when operated at a high perturbation rate

The step irradiance decrease can be experimentally emulated by disconnecting one of the two parallel sections of the PV array while the system is running, mimicking a 50% step decrease in solar irradiance. When an array branch is disconnected at an irradiance level of 859.8W/m^2 and a cell temperature of 39.6˚C, the algorithm takes less than 1s to respond to the branch disconnection (Fig. 9b). Even with the non-periodic fluctuations in the array voltage and current waveforms, the corresponding drop in array power below its maximum value is very low, resulting in a high tracking efficiency. At low perturbation rates the algorithm takes much longer to respond to a branch disconnection at similar weather conditions (Fig. 9a). As shown, the array voltage drops to a lower value in the region of 109V compared to about 132V when using the higher perturbation rate. In obtaining these results, algorithm parameters were set to their optimum three-level operation values as discussed in [8]. The simulation and experimental results presented in Figs. 8-9 show that the INC algorithm performs better at rapidly changing irradiance when employed with a high perturbation rate.

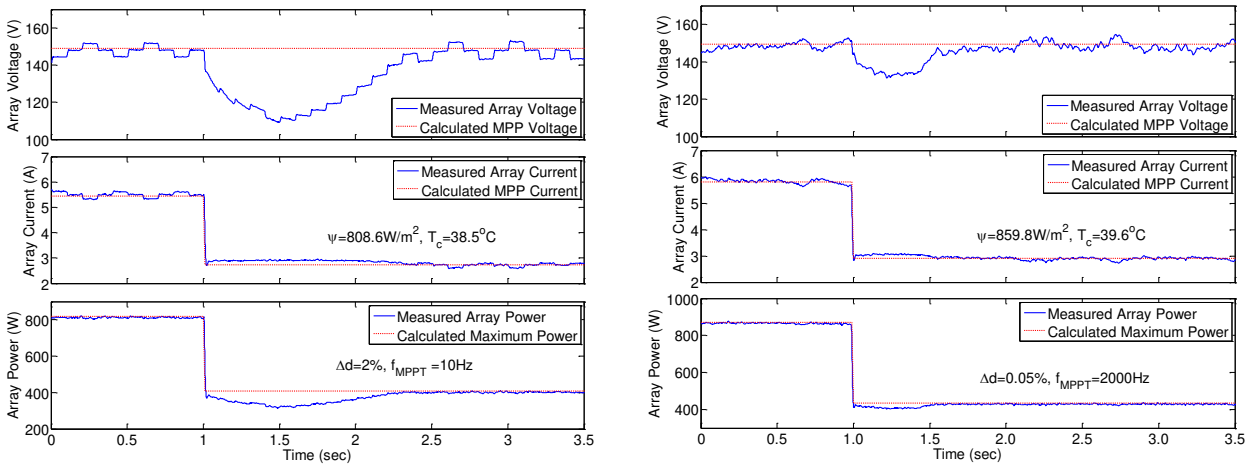

(a) (b)

Fig. 9. Experimental results showing the array current, voltage and power following the disconnection of an array branch; (a) three-level operation, (b) high perturbation rate.

7. Energy Utilization

At a particular set of algorithm parameters and for a given PV array size, the energy utilization efficiency of an MPPT algorithm depends on weather conditions, the time constant of the system and converter design in terms of noise immunity. Higher levels of energy utilization can normally be achieved at higher irradiance levels since the perturbation in the control parameter produces a higher array power change magnitude and consequently less algorithm confusion. At lower irradiance levels, the power-voltage curve is more flat and the change in array power due to an algorithm perturbation becomes comparable to that caused by noise. This leads to algorithm confusion and lower energy utilization efficiency.

For an actual site installation such as the one considered in this study, control of the irradiance level is not possible as would be the case in simulation or when using a PV emulator under laboratory test conditions. The energy utilization efficiency of this experimental system was therefore calculated for 20 min operation periods at different weather conditions during periods of

both slowly changing irradiance and rapidly changing irradiance conditions. The perturbation rate of the INC algorithm was set to be equal to the ADC rate (2kHz) and the step size was set at an appropriate value of 0.05% (as discussed in Section 4). The calculated energy utilization efficiency for the slow changing irradiance shown in Fig. 10a is about 97.4%. A higher energy utilization efficiency of 98.8% was obtained for the rapidly changing irradiance conditions shown in Fig. 10b. This higher energy utilization efficiency is due to the presence of long intervals of high-level irradiance where the change in duty ratio has a considerable effect on array power leading to less algorithm confusion. At low irradiance levels, the PV array has a low dP_{PV}/dV_{PV} resulting in wider swings in array voltage. This did not have a significant effect on the energy utilization efficiency since the maximum energy that can be drawn from the PV array under these conditions is low.

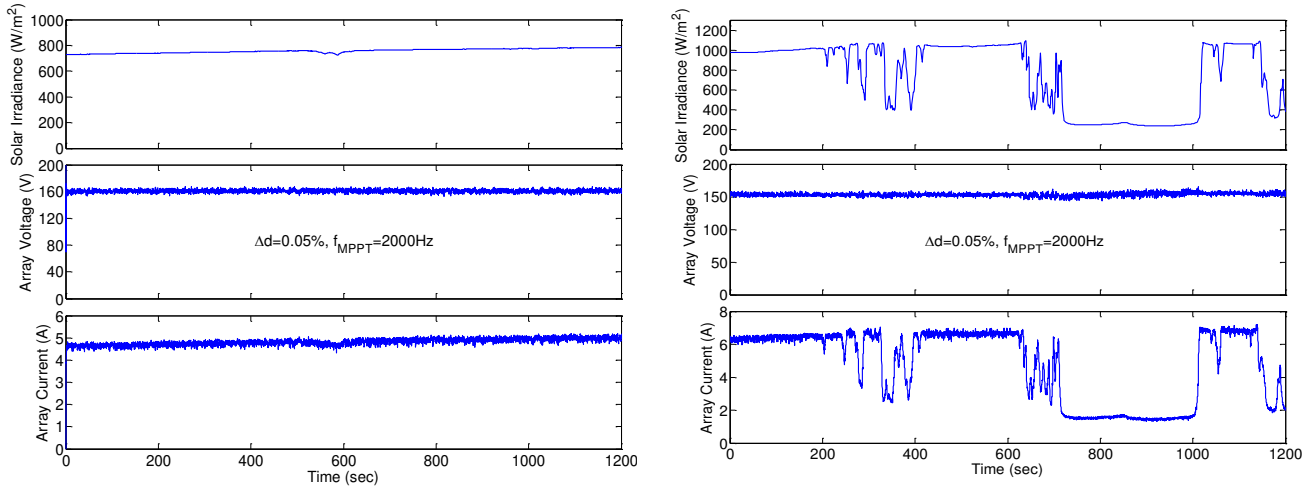

(a) (b)

Fig. 10. Experimental system performance with a high perturbation rate; (a) slow changing irradiance, (b) rapidly changing irradiance.

At high perturbation rates, the INC algorithm recovers the correct perturbation direction quickly after confusion due to noise or irradiance changes. This yields slightly higher energy utilization efficiencies compared to three-level operation at lower perturbation rates, especially for rapidly

changing irradiance. For example, with the optimum 3-level operating parameters [8], the calculated energy utilization efficiency for the rapidly changing irradiance was about 96.8%, lower than the 98.8% obtained using the high perturbation rate. The algorithm is more confused at rapidly changing irradiance during low irradiance intervals when operated in three-level mode using a low perturbation rate of 10Hz. Although the above tests were carried out at different irradiance levels (as irradiance levels cannot be controlled in a site PV installation), they however give an indication of the excellent performance of the INC algorithm when operated at high perturbation rates. Table 1 shows a comparison of the INC algorithm characteristics when operated at a high perturbation rate with previously published results obtained with conventional three-level operation of the algorithm using the same standalone PV system considered in this paper.

Table 1. Comparison between low and high perturbation rate operation of the INC MPPT algorithm

	Three-level operation [8]	**High perturbation rate operation**
Measured parameters	V_{PV}, I_{PV}	V_{PV}, I_{PV}
Perturbation Parameter	*Vref , Iref or D*	*D only*
Decision Based on change in	V_{PV} and I_{PV}	V_{PV} and I_{PV}
Implementation cost	low	slightly higher
Steady-state fluctuations in array voltage	three-level	quasi-periodic
Convergence speed	relatively slow	fast
Dependence of tracking efficiency on cell temperature and irradiance levels	less dependent	more dependent
Tracking efficiencies for stationary weather conditions	high	higher

Tracking efficiencies for rapidly changing irradiance	relatively low	high
Confusion due to noise	less affected	more affected
Confusion due to system dynamics	less affected	more affected
Confusion due to irradiance changes	more affected	less affected
Tracking efficiency for experimental system; reference voltage control	95% - 98%	N/A
Tracking efficiency for experimental system; duty ratio control	96% - 99%	97% - 99%

8. Conclusion

The paper evaluates, for the first time, the qualitative and quantitative behavior of the INC MPPT algorithm when employed at a high perturbation frequency. Simulation and experimental results of standalone PV systems with a motor-pump load and a resistive load have been used in this investigation. The performance of the INC algorithm in this operation mode is compared with that of its conventional three-level mode of operation at the same high perturbation frequency, using the same standalone PV system.

At high perturbation rates, the system is never allowed to reach a steady state and the interaction between system dynamics and the INC algorithm perturbations results in quasi-periodic waveforms. However, the waveforms of the system are always bounded and the system is globally stable. With high perturbation rates, the INC algorithm offers faster transient response and lower steady-state oscillation compared to conventional three-level mode of operation. It also offers faster recovery of the MPP when the algorithm is confused due to noise or irradiance changes. These characteristics mean that the INC algorithm delivers higher energy utilization efficiencies when operated at a high perturbation rate.

References

[1] de Brito, M.A., Galotto, L., Sampaio, L.P., de Azevedo e Melo, G., Canesin, C.A.: 'Evaluation of the main MPPT techniques for photovoltaic applications', IEEE Transactions on Industrial Electronics, 2013, 60, (3), pp. 1156–1167

[2] Subudhi, B., Pradhan, R.: 'A comparative study on maximum power point tracking techniques for photovoltaic power systems', IEEE Transactions on Sustainable Energy, 2013, 4, (1), pp. 89-98

[3] Kish, G.J., Lee, J.J., Lehn, P.W.: 'Modelling and control of photovoltaic panels utilising the incremental conductance method for maximum power point tracking', IET Renewable Power Generation, 2012, 6, (4), pp. 259-266

[4] Faraji, R., Rouholamini, A., Naji, H.R., Fadaeinedjad, R., Chavoshian, M.R.: 'FPGA-based real time incremental conductance maximum power point tracking controller for photovoltaic systems', IET Renewable Power Generation, 2014, 7, (5), pp. 1294 – 1304

[5] Sekhar, P.C., Mishra, S.: 'Takagi–Sugeno fuzzy-based incremental conductance algorithm for maximum power point tracking of a photovoltaic generating system', IET Renewable Power Generation, 2014, 8, (8), pp. 900 – 914

[6] Brunton, S.L., Rowley, C.W., Kulkarni, S.R., Clarkson, C.: 'Maximum power point tracking for photovoltaic optimization using ripple-based extremum seeking control', IEEE Transactions on Power Electronics, 2010, 25, (10), pp. 2531-2539

[7] Sera, D., Mathe, L., Kerekes, T., Spataru, S., Teodorescu, R.: 'On the perturb-and-observe and incremental conductance MPPT methods for PV systems', IEEE Journal of Photovoltaic, 2013, 3, (3), pp. 1070–1078

[8] Elgendy, M.A., Zahawi, B., Atkinson, D.J.: 'Assessment of the incremental conductance maximum power point tracking algorithm', IEEE Transactions on Sustainable Energy, 2013, 4, (1), pp. 108-117

[9] Hussein, K.H., Muta, I., Hoshino, T., Osakada, M.: 'Maximum photovoltaic power tracking: an algorithm for rapidly changing atmospheric conditions', IEE Proceedings: Generation, Transmission and Distribution, 1995, 142, (1), pp. 59-64

[10] Kjær, S.: 'Evaluation of the hill climbing and the incremental conductance maximum power point trackers for photovoltaic power systems', IEEE Transactions on Energy Conversion, 2012, 27, (4), pp. 922-929

[11] Safari, A., Mekhilef, S.: 'Simulation and hardware implementation of incremental conductance MPPT with direct control method using Cuk converter', IEEE Transactions on Industrial Electronics, 2011, 58, (4), pp. 1154 - 1161

[12] Liu, F., Duan, S., Liu, F., Liu, B., Kang, Y.: 'A variable step size INC MPPT method for PV systems', IEEE Transactions on Industrial Electronics, 2008, 55, (7), pp. 2622-2628

[13] Ahmed, A., Ran, L., Moon, S., Park, J.-H.: 'A fast PV power tracking control algorithm with reduced power mode', IEEE Transactions on Energy Conversion, 2013, 28, (3), pp. 565–575

[14] Mei, Q., Shan, M., Liu, L., Guerrero, J.M.: 'A novel improved variable step-size incremental-resistance MPPT method for PV systems', IEEE Transactions on Industrial Electronics, 2011, 58, (6), pp. 2427-2434

[15] Lee, K.-J., Kim, R.-Y.: 'An adaptive maximum power point tracking scheme based on a variable scaling factor for photovoltaic systems', IEEE Transactions on Energy Conversion, 2012, 27, (4), pp. 1002 – 1008

[16] Elgendy, M.A., Zahawi, B., Atkinson, D.J.: 'Operating characteristics of the P&O algorithm at high perturbation frequencies for standalone PV systems', IEEE Transactions on Energy Conversion, 2015, 30, (1), pp. 189-198

[17] Elgendy, M.A., Zahawi, B., Atkinson, D.J.: 'Assessment of perturb and observe MPPT algorithm implementation techniques for PV pumping applications', IEEE Transactions on Sustainable Energy, 2012, 3, (1), pp. 21-33

[18] Elgendy, M.A., Zahawi, B., Atkinson, D.J.: 'Comparison of directly connected and constant voltage controlled photovoltaic pumping systems', IEEE Transactions on Sustainable Energy, 2010, 1, (3), pp. 184-192

[19] Tse, C.K.: 'Complex behavior of switching power converters' (London: CRC Press, 2003)

[20] Hamill, D.C., Banerjee, S., Verghese, G.C.: 'Nonlinear phenomena in power electronics; attractors, bifurcations, chaos, and nonlinear control' (John Wiley and Sons, Hoboken, NJ, 2001)